Geoscience Frontiers xxx (2018) 1–14

HOSTED BY

Contents lists available at ScienceDirect

China University of Geosciences (Beijing)

Geoscience Frontiers

journal homepage: www.elsevier.com/locate/gsf

Research Paper

The impact of crustal rheology on natural seismicity: Campi Flegrei caldera case study

R. Castaldo [a], L. D'Auria [b,c], S. Pepe [a], G. Solaro [a], V. De Novellis [a], P. Tizzani [a,*]

[a] Istituto per il Rilevamento Elettromagnetico dell'Ambiente (IREA)-Consiglio Nazionale delle Ricerche (CNR), Napoli, Italy
[b] Instituto Volcanológico de Canarias (INVOLCAN), Puerto de la Cruz, Tenerife, Spain
[c] Instituto Tecnológico y de Energías Renovables (ITER), Granadilla de Abona, Tenerife, Spain

ARTICLE INFO

Article history:
Received 16 June 2017
Received in revised form
11 December 2017
Accepted 11 February 2018
Available online xxx
Handling Editor: Masaki Yoshida

Keywords:
Brittle-ductile transition
Seismicity cut-off
Geothermal measurements
FE conductive thermal modelling
Campi Flegrei caldera

ABSTRACT

We analyze the crustal rheology beneath the active resurgent Campi Flegrei caldera (CFc) in Southern Italy by modelling the 3D brittle-ductile (B/D) transition, based on available thermal, geological and geophysical data. Firstly, the thermal field in the conductive physical regime is modeled using a finite element method; based on an optimization tool, this method is applied to evaluate the location and dimensions of the deep thermal source beneath the caldera. A horizontally-extended thermal anomaly located at about 5000 m depth below sea level is identified beneath Pozzuoli Bay, a part of the CFc. The same isotherm is located at a depth of 20,000 m beyond the caldera. This indicates a higher horizontal temperature gradient in the caldera with respect to the surrounding area. Next, we utilize this thermal model to image the 3D rheological stratification of the shallow crust below the caldera with two different values of strain rates. Within the caldera, the B/D transitions with ε equal to 10^{-12} s^{-1} and 10^{-8} s^{-1} are located at 3000 m and 5000 m depths, respectively. Outside the caldera, the transition is very deep (15,000–20,000 m), seemingly uninfluenced by the thermal state of the CFc volcanism. Finally, we compare these results with the spatial distribution of earthquake hypocenters, Benioff strain release and b-value distribution to investigate the relationship between crustal rheology and seismicity characteristics. Our analysis reveals that the image of the B/D transition is in agreement with the distribution of earthquake hypocenters, constraining the potential seismogenic volume of the region. Our study demonstrates that knowledge of the rheological state of a volcanic system is an important element to interpret its dynamic, forecast future activity and improve evaluation of the associated seismic hazard.

1. Introduction

The last decade saw significant advances in our understanding of the rheology of rocks and associated geological processes. The thermo-rheology of rocks is a crucial factor in understanding the mechanical behavior of the crust in tectonically active areas (Ord and Hobbs, 1989). Several studies have been performed in order to understand the role of the thermal state of the crust plays in the evolution of volcanic areas (Ito, 1993).

In this work, we analyze the crustal rheology of the Campi Flegrei caldera (CFc), a high hazard volcanic area comprising part of the Naples metropolitan area (Italy) and thus threatening about 1.5 million people. The CFc is a thermally-active Quaternary resurgent caldera (Chiodini et al., 2010) located within the Campanian Plain, which is a graben-like structure at the eastern margin of the Tyrrhenian Sea (Luongo et al., 1991). The current CFc landscape was shaped by two main explosive eruptions, the older of which occurred about 40 kyrs ago (Di Vito et al., 1999; Scarpati et al., 2013) and erupted about 100 km^3 of Dense Rock Equivalent (DRE) (Wohletz et al., 1999), producing a thick layer up to 100 m, called Campania Ignimbrite (CI). The younger explosive eruption is dated at about 15 kyrs and erupted about 50 km^3 of DRE producing a thick tuff, called Neapolitan Yellow Tuff (NYT) (Wohletz et al., 1999; Smith et al., 2011) (Fig. 1). The last eruption of the CFc occurred in 1538; it was mainly phreatomagmatic (Smith et al., 2011) and formed a 150 m high spatter cone, called Mt. Nuovo. Currently, the caldera is affected by significant deformation, characterized by episodes of inflation and deflation, which appear to have a rough

* Corresponding author.
E-mail address: tizzani.p@irea.cnr.it (P. Tizzani).
Peer-review under responsibility of China University of Geosciences (Beijing).

https://doi.org/10.1016/j.gsf.2018.02.003

Please cite this article in press as: Castaldo, R., et al., The impact of crustal rheology on natural seismicity: Campi Flegrei caldera case study, Geoscience Frontiers (2018), https://doi.org/10.1016/j.gsf.2018.02.003

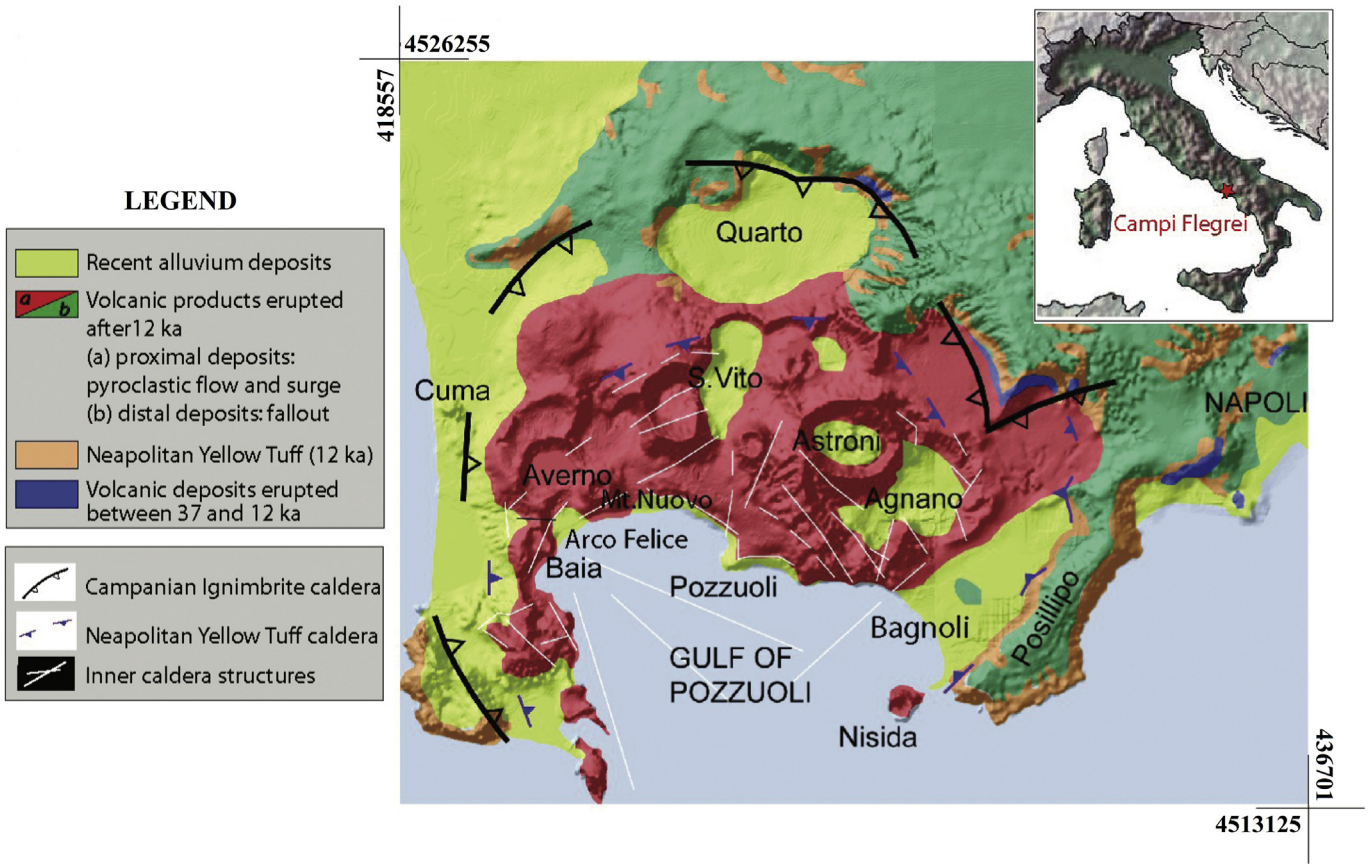

Figure 1. Geology of the CFc. Simplified geological map imposed on a shaded relief DEM of the area. Inset in the upper right corner shows the location of the study area.

circular symmetry of about 6000 m radius; there are no macroscopic differences of shape and size between episodes (Avallone et al., 1999; Orsi et al., 1999; Lundgren et al., 2001). In the last 70 years, the CFc has undergone at least three episodes of major uplift. The first episode occurred between 1950 and 1952, and resulted in a total uplift of about 0.7 m. This episode was not accompanied by significant levels of seismicity (Del Gaudio et al., 2010). The second episode, between 1968 and 1972, resulted in an uplift of about 1.77 m accompanied by moderate seismicity ($M < 2.5$). The third episode (1982–1984) had a total uplift of about 1.8 m and was characterized by intense seismicity, with more than 16,000 earthquakes having magnitudes up to 4.2 (D'Auria et al., 2011 and references therein). The seismicity of the last episode was recorded by dense seismic networks, allowing accurate hypocenter locations; most of these earthquakes occurred at shallow depths (less than 3000 m). Spatial distribution of the strain release showed marked concentration around the Solfatara crater. Clusters of earthquakes were also located beneath the town of Pozzuoli and the Pozzuoli Bay (D'Auria et al., 2011; De Siena et al., 2017).

The thermal field data indicate a significant anomaly in the caldera, with a temperature of about 400 °C measured at 3000 m depth. Moreover, surface geothermal gradients from shallow boreholes showed a value of 3–4 Heat Flux Unit (HFU) (Corrado et al., 1998). Seismic wave attenuation studies corroborate these findings and provide an overall picture of the thermal regime in the upper crust of the caldera (De Lorenzo et al., 2001).

The possible presence of a magma reservoir at about 5000 m depth is suggested by the identification of a P-SV converted phase in a seismic profile (Ferrucci et al., 1992), by the maximum depth of earthquakes (De Natale et al., 1995), and by petrological and geochemical data (Civetta et al., 1991). Previous studies document the existence of a magma chamber beneath the caldera (Rosi and Sbrana, 1987; Villemant, 1988; Civetta et al., 1991; Trasatti et al., 2008), and that it is likely located at shallow depth 4000–5000 m (Ortiz et al., 1984; Berrino et al., 2008). More recently, De Siena et al. (2017) suggested an area of high-attenuation between 4000 and 4500 m depth. In addition, petrological and isotopic data show that the magmatic system, before the NYT eruption, was refilled by variable-sized batches of magma (D'Antonio et al., 1999; Pappalardo et al., 1999).

In order to investigate the shape of the magmatic source responsible of the high thermal gradient observed at the CFc, Wohletz et al. (1999) and Orsi et al. (1999) performed 2D numerical simulations to account for conductive and convective heat transfer in magma reservoirs of various sizes, by taking into consideration actual thermal measurements. They verified that the contribution of convective heat transfer is enough to justify the temperature variations with depth observed in geothermal wells distributed across the caldera (Agip, 1987).

Despite many studies that focus on imaging the internal structure of the CFc, the 3D thermo-rheological stratification of the crust below the caldera has not yet been adequately described. To bridge this gap, we model the 3D brittle-ductile (B/D) transition through an analysis of thermal, geological and geophysical data. We first perform a 3D finite element (FE) modelling of the conductive thermal field by using a priori geological and geophysical information. With a Monte Carlo search method, we then define the dimensions and location of the deep thermal source beneath the

Please cite this article in press as: Castaldo, R., et al., The impact of crustal rheology on natural seismicity: Campi Flegrei caldera case study, Geoscience Frontiers (2018), https://doi.org/10.1016/j.gsf.2018.02.003

caldera, and image the 3D rheological stratification of the shallow crust with the retrieved thermal model. Finally, we compare our results with the spatial distribution of hypocenters, Benioff strain release and b-value distribution, to evaluate the relationship between crust rheology and natural seismicity. Our analysis revealed that the image of the B/D transition has an important implication in constraining the seismicity distribution and the potential seismogenic volume of the area.

2. Data input

The CFc region has been intensively explored for nearly a century to evaluate the geothermal potential of the Neapolitan volcanic district. Initial geothermal explorations in the CFc were carried out by the SAFEN Company in 1939 and 1953. The company drilled several wells with depths ranging from a few meters to 600 m near Mofete, west of Pozzuoli City (Fig. 2). Shallow drilling demonstrated regional potential geothermal energy extraction, with temperatures of about 200 °C at depths of 500 m. These high temperatures stimulated further interest in geothermal research, which led to the development of a new regional drilling program, carried out between 1977 and 1985, by the AGIP-ENEL joint venture (Agip, 1987; Carlino et al., 2013). Geothermal gradients were measured in seven boreholes drilled as part of the AGIP-ENEL joint venture and two SAFEN deep geothermal boreholes (Fig. 2) (Agip, 1987; Bianchi et al., 1987). These drill sites are located in three main areas: Mofete, Licola, and San Vito (Fig. 2a). Thermal measurements indicate that the highest gradients are found at Mofete, where hydrothermal activity has been observed (De Vivo et al., 1989; Chiodini et al., 2010; Mormone et al., 2015). This effect is less apparent at San Vito and completely absent at Licola, drilled outside the caldera margin.

Subsequently, Corrado et al. (1998) proposed a heat flow density map of the CFc made by considering thermal measurements carried out in 30 shallow water wells (up to 140 m deep). We extrapolated heat flow values corresponding to the nine boreholes from Corrado et al. (1998), and also evaluated the heat flow value at the Mt. Nuovo measurement point, in the absence of a thermal deep borehole (Fig. 2a).

In order to calibrate the 3D FE thermal model of the crust beneath the CFc through the Monte Carlo optimization procedure, we consider available thermal measurements of the area from nine deep geothermal boreholes and ten heat flow measurement points (Fig. 2b, Section 3). Conductive thermal modelling is performed on numerical domains that include the Campania Ignimbrite caldera and the surrounding areas, to a crustal depth of 20,000 m. The model is built up by integrating the available geological and geophysical information. To assess mechanical properties of the crust, we take into account the shallow lithological succession obtained in a seismic tomography study by Chiarabba and Moretti (2006) and gravimetric inversion, presented by Berrino et al. (2008). To define the Moho depth, we consider the model proposed by Ferrucci et al. (1986), which shows a crust/mantle transition at a depth of less than 25,000 m. We evaluate the data distribution in the volume through a gridding technique that allows interpolation of scattered data points into a uniform lattice. We obtained the 3D density and thermal parameters (thermal conductivity k and specific heat capacity distribution Cp, reported in Table 1; Wohletz et al., 1999; and reference within) distribution by using inverse distance weighting (IDW), a deterministic method for multivariate interpolation of a set of scattered points (Goovaerts, 1997). Thermal conductivity values are calculated by considering the Chapman and Furlong (1992) equation, in order to take into account their dependence on temperature and depth. The results of the multivariate interpolation are displayed in Fig. 3a.

3. 3D thermal FE model

In order to investigate the thermal state of the first 20,000 m beneath the CFc, we executed a stationary 3D FE model in a conductive physical regime, excluding the convective heat component that is confined to the shallow hydrothermal system. We support the initial assumption of stationary propagation of a thermal wave by computing the thermal wavelength that propagates in a medium having the same physical properties as the CFc. For a period of about 40 kyrs BP (i.e. dating the CI eruption as representative of the main thermal climax event), the calculated thermal wavelength is about 1000 m (Turcotte and Schubert, 2002). Thus, measured data does not support detailed time-varying models; the wavelength propagation due to high frequency thermal events (i.e., for an event that occurred about 4 kyrs BP) is too small to affect the shallowest portion of the crust (first 2000–4000 m of depth), where the data are recorded.

In this physical scenario, following Fourier's law, we consider heat transfer to be stationary. Hence, the governing equations to solve our problem in a conductive regime are:

$$\rho \cdot Cp \cdot \nabla T = -\nabla \cdot \vec{q} + Q \quad (1)$$

where ρ (kg/m^3) is the density of the rocks, C_p is the specific heat capacity (J/kg K), T is the absolute temperature (K), $\vec{q}$ (W/m^2) is the conductive heat flux vector and Q is the volumetric heat source production (W/m^3). The conductive heat flux vector is represented by:

$$\vec{q} = -k\nabla T \quad (2)$$

where k (W/m K) is the thermal conductivity.

The initial model setting is implemented by considering crustal heterogeneities presented in the previous section (Fig. 3a). We define the 3D domain in which mechanical and thermal heterogeneities are included as functions $F(x,y,z)$ with a 500 m × 500 m resolution. The computational domain is characterized by a size of 38,000 m × 32,000 m × 20,000 m in the east, north and vertical directions, respectively. Subsequently, we defined the mesh domain, discretizing the 3D geometry with about 45,360 tetrahedral elements, characterized by maximum and minimum sides equal to 1500 m and 500 m, respectively, and using a cubic shape function. A finer mesh would have improved the results by less than 5% (Zhang and Zhu, 1998). The geothermal gradient of $dT/dz \approx 30$ °C/km is used to set the initial values of crustal temperature (Fig. 3b). Following the results from Wohletz et al. (1999) and considering the gravimetric data interpretation (Fedi et al., 1991; Berrino et al., 2008), we assume an oblate spheroid as the heat source, that simulates well the geometry of a funnel-shaped magma chamber with a flat top; its surface temperature is fixed at 880 °C, based on temperatures reached in a rhyolitic magmatic chamber (Chiodini et al., 2016).

As boundary conditions, we consider: (1) outgoing heat, flowing from the upper part of the computational domain, i.e., the ground surface; (2) temperature, set by the continental geothermal gradient bounding the four sides of the domain; and (3) an inner heat flux condition at the bottom of the domain (20,000 m depth), according to the Moho heat flow (Fig. 3b).

Following Castaldo et al. (2017), we propose an optimization procedure based on minimization of the difference between the FE model predictions and observations (i.e., residuals), which are derived by the heat flow and thermal borehole data. We combine benefits of FE environments with the Monte Carlo optimization method (Sen and Stoffa, 2013) to evaluate geometric source parameters related to the oblate spheroid located beneath the CFc. Following this procedure, several forward models that depend upon

Please cite this article in press as: Castaldo, R., et al., The impact of crustal rheology on natural seismicity: Campi Flegrei caldera case study, Geoscience Frontiers (2018), https://doi.org/10.1016/j.gsf.2018.02.003

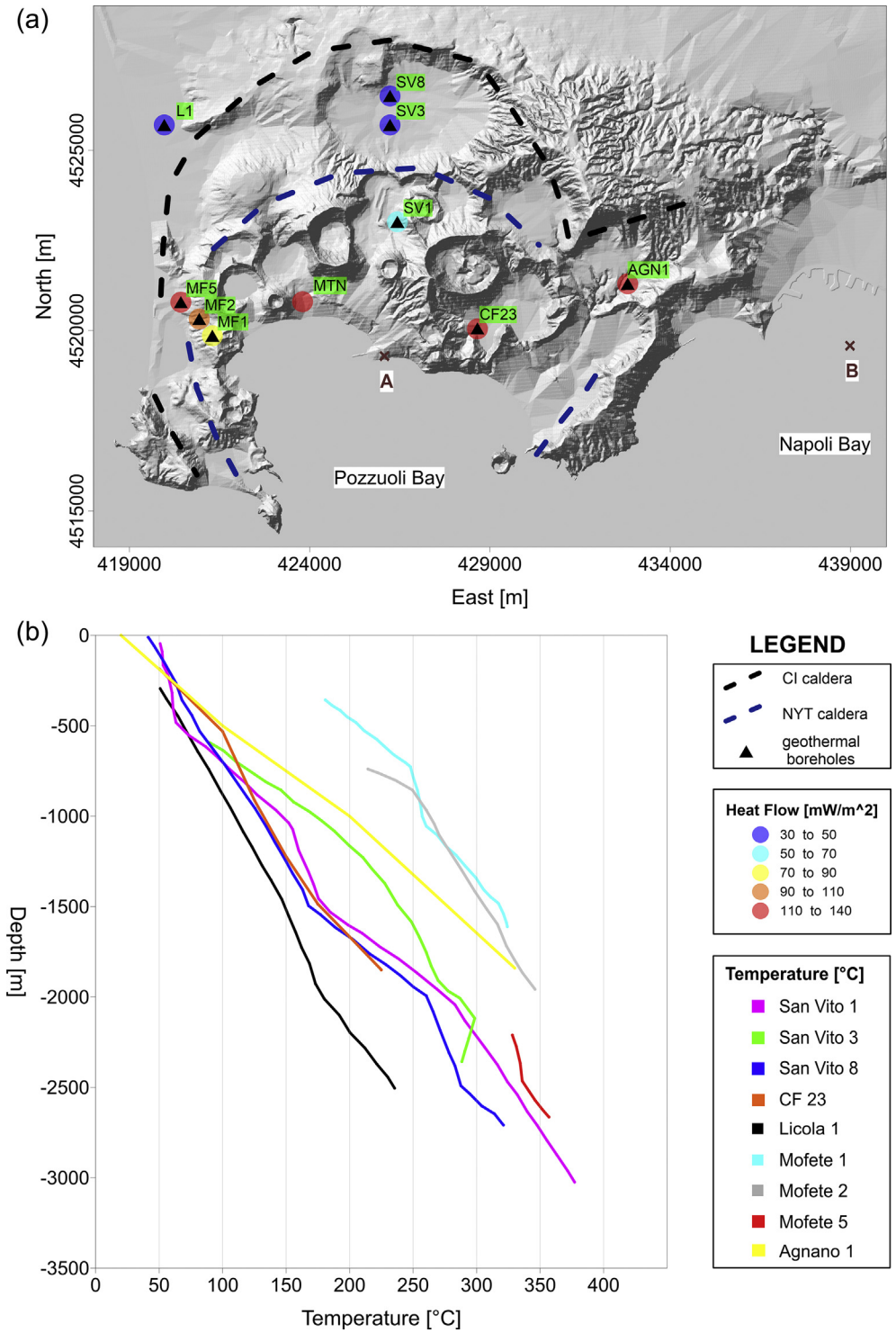

Figure 2. Thermal data. (a) Location of geothermal boreholes (black triangles) (Agip, 1987; Carlino et al., 2013) and heat flow measurement points (colored circles) (Corrado et al., 1998) imposed on the CFc SRTM DEM. The black and blue dotted lines (also marked in Fig. 1) indicate the borders of the two explosive caldera-forming eruptions, the Campanian Ignimbrite (CI) and Neapolitan Yellow Tuff (NYT), respectively (Orsi et al., 1999). Points A and B indicate the location of the rheological vertical profiles reported in Fig. 6a. (b) Vertical temperature profiles for geothermal boreholes considered in this study are shown (Agip, 1987; Carlino et al., 2013).

oblate spheroid geometric source parameters are executed; the source parameters are the major (a) and minor (c) axes of the oblate spheroid representing the heat source, and the depth of its center (z_c). These three parameters are targets of the optimization procedure and are examined over a combination of values within the bounding volume of the computational domain (Table 2). The best-fit solution is selected from among 350 forward models, on the basis of a simple Root Mean Squared Error (RMSE) criterion. The results of quantitative comparisons between the optimized model, geothermal borehole and heat flow measurements are shown in Fig. 4 and Supplementary Table S1, respectively. Fig. 4a shows a general good agreement between thermal data and model results, except for the

Please cite this article in press as: Castaldo, R., et al., The impact of crustal rheology on natural seismicity: Campi Flegrei caldera case study, Geoscience Frontiers (2018), https://doi.org/10.1016/j.gsf.2018.02.003

Table 1
Density and thermal parameters (Chelini and Sbrana, 1987; Wohletz et al., 1999) of rock successions.

Rocks	Density (kg/m^3)	Specific heat capacity (J/kg K)	Thermal conductivity (W/m K)
Polygenic tufites	2300	600	1.5
Magmatic chamber	2500	900	3
Carbonate bedrock	2600	850	2.5
Crystalline metamorphic	2800	1000	2
Upper mantle	3000	1100	1.5

Table 2
Geometric model parameters: bounding of unknown parameters (a: major axis; c: minor axis; z_c: center of depth) and the estimated values.

Parameters	Lower bound (m)	Upper bound (m)	Estimated value (m)
z_c	−9000	−3000	−5400
a	4000	10,000	7000
c	200	1500	900

Mofete boreholes (MF1 and MF2), where a major discrepancy was found. The heat flow values also show high discrepancy with respect to modeled estimates in the Mofete and Agnano thermal areas (Supplementary Table S1). These differences could be explained as: (1) the effect of shallow hydrothermal activity suggested by mineralogical studies (De Vivo et al., 1989; Chiodini et al., 2010; Mormone et al., 2015), (2) lateral variations in the thermal conductivity distribution used in our model (Wohletz et al., 1999; Carlino et al., 2013), and (3) the impact of an advective component on the thermal state, likely due to the existence of structures at the boundary of the NYT caldera, which could explain the anomalous behavior with respect to our conductive model results.

The estimated best source geometric parameters are reported in Table 2. The retrieved values indicate a heat source extending horizontally for about 7000 m, with a flat top and located at about 5000 m depth.

In Fig. 5, the retrieved 3D distribution of temperature beneath the CFc is shown. The results of the FE conductive thermal model show a thermal anomaly beneath the Pozzuoli Bay, with temperature values of about 800 °C, located at a depth of 5000 m below sea level. The same isotherm, located at a depth of 20,000 m outside the CFc, indicates a higher horizontal gradient of temperature in the CFc with respect to the surrounding area. The upper surface of the 3D image depicts the heat flow map.

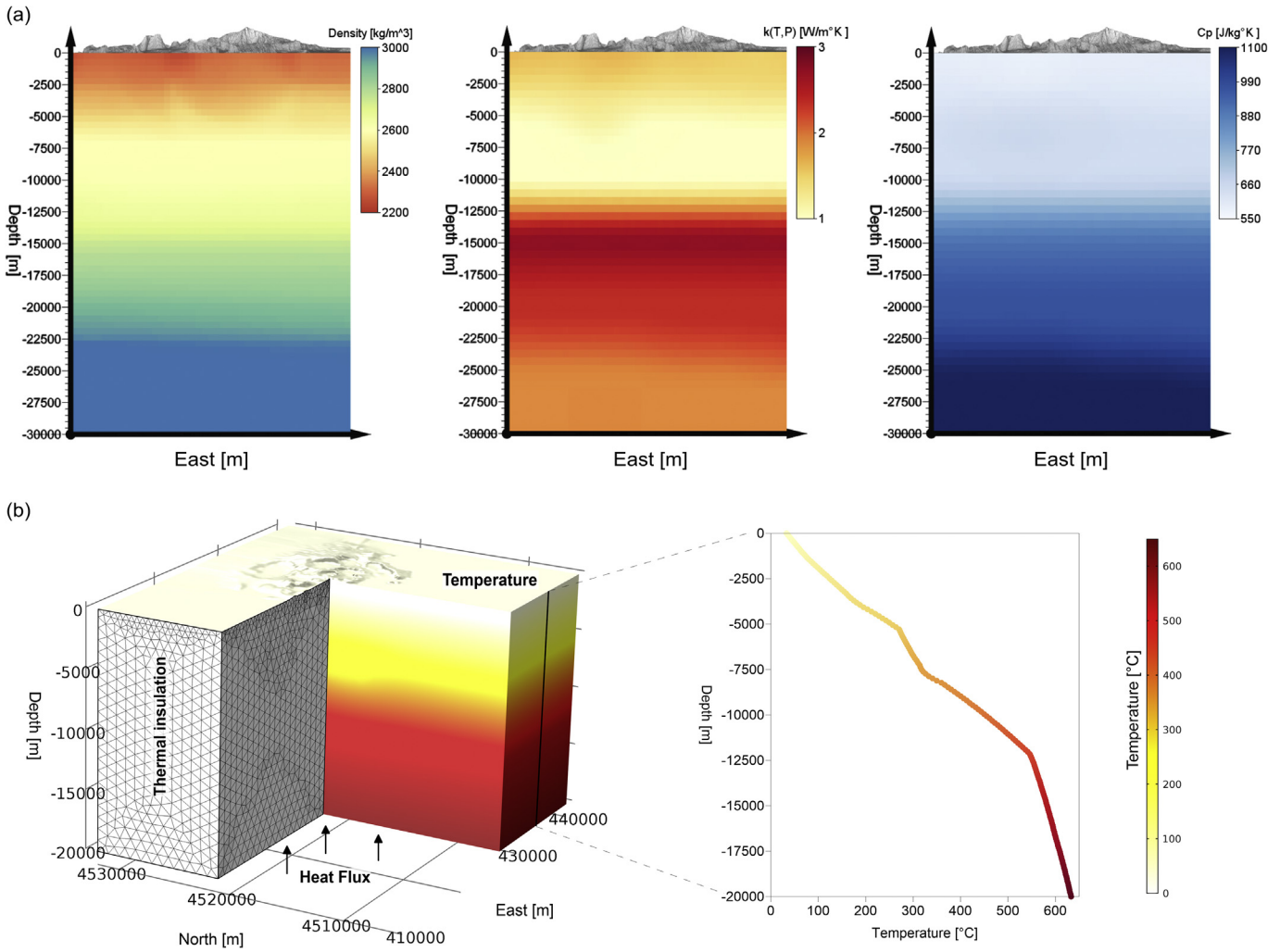

Figure 3. Input parameters of FE modelling. (a) From left: density, thermal conductivity (k) and specific heat capacity distribution (C_p) beneath the CFc, respectively (Chapman and Furlong, 1992; Wohletz et al., 1999; Chiarabba and Moretti, 2006; Berrino et al., 2008). (b) Discretized model domains through tetrahedral elements and boundary conditions applied in the FE analysis. The vertical profile represents the initial temperature of the model.

Please cite this article in press as: Castaldo, R., et al., The impact of crustal rheology on natural seismicity: Campi Flegrei caldera case study, Geoscience Frontiers (2018), https://doi.org/10.1016/j.gsf.2018.02.003

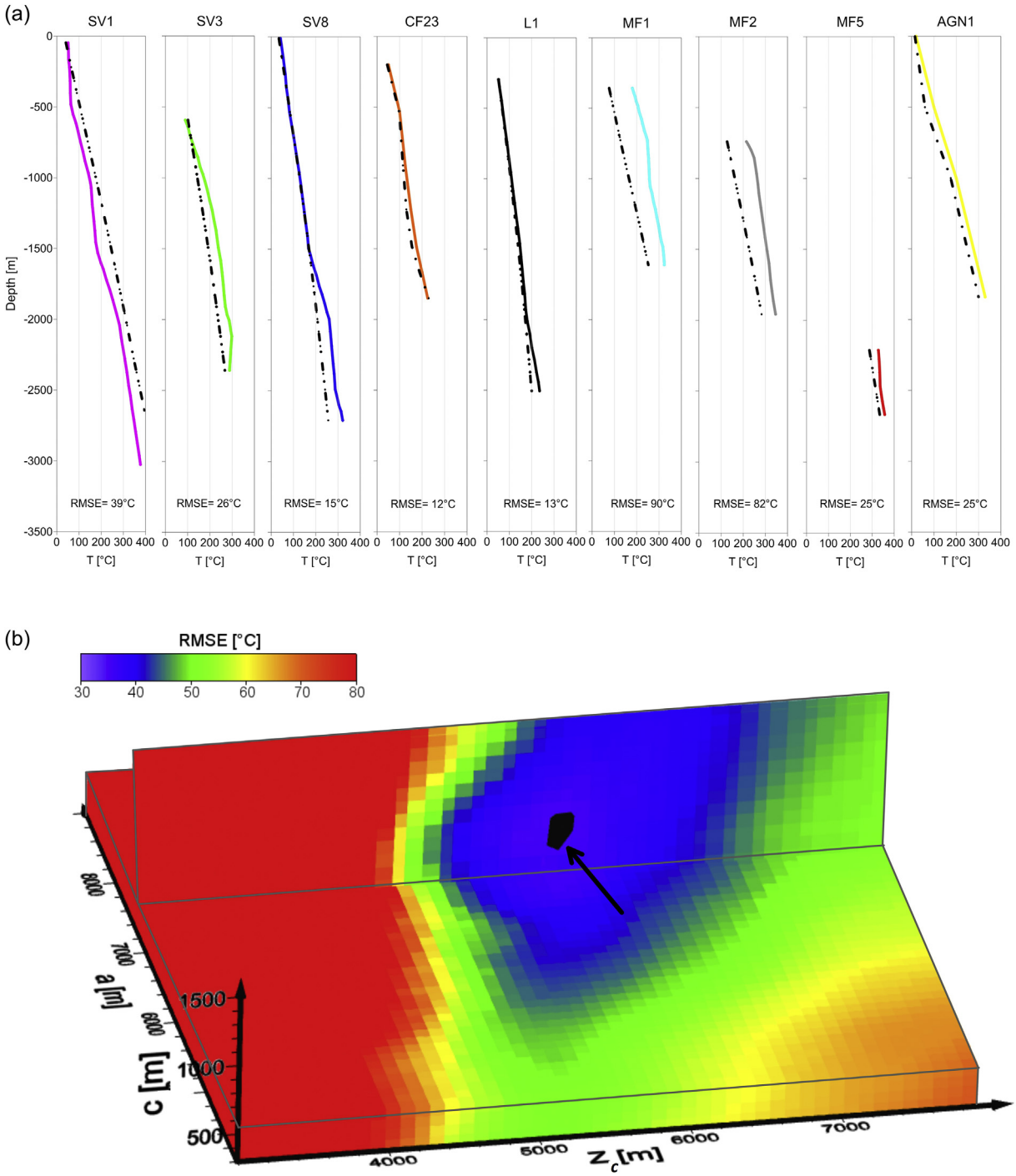

Figure 4. FE model results 1: comparative analysis. (a) Comparison between measured (colored lines) and model (point dashed lines) data for different geothermal boreholes (see their locations in Fig. 2); for each geothermal borehole, we report RMSE values. (b) Results of three-dimensional distribution of RMSE values evaluated for each model were obtained by varying geometric source parameters (a: major axis; c: minor axis; z_c: depth of center). The black region represents the minimum RMSE (37 °C), corresponding to the best source geometric parameters.

4. Rheological model and natural seismicity

The concept of a rheological profile was first developed by Goetze and Evans (1979), assuming that the deformation regimes for any given rock can be subdivided into two domains: brittle (B) and ductile (D). The B/D transition in the crust is thought to be related to the seismic-aseismic boundary. The thickness of the seismogenetic layer and consequent regional variations in the cut-off depth of seismicity are closely related to the strength of the crust (Meissner and Strehlau, 1982).

Brittle behaviour is generally expressed by a linear friction failure law, proposed by Sibson (1974):

$$(\sigma_1 - \sigma_3)_B = \beta \cdot \rho \cdot g \cdot z \cdot (1 - \lambda) \quad (5)$$

Please cite this article in press as: Castaldo, R., et al., The impact of crustal rheology on natural seismicity: Campi Flegrei caldera case study, Geoscience Frontiers (2018), https://doi.org/10.1016/j.gsf.2018.02.003

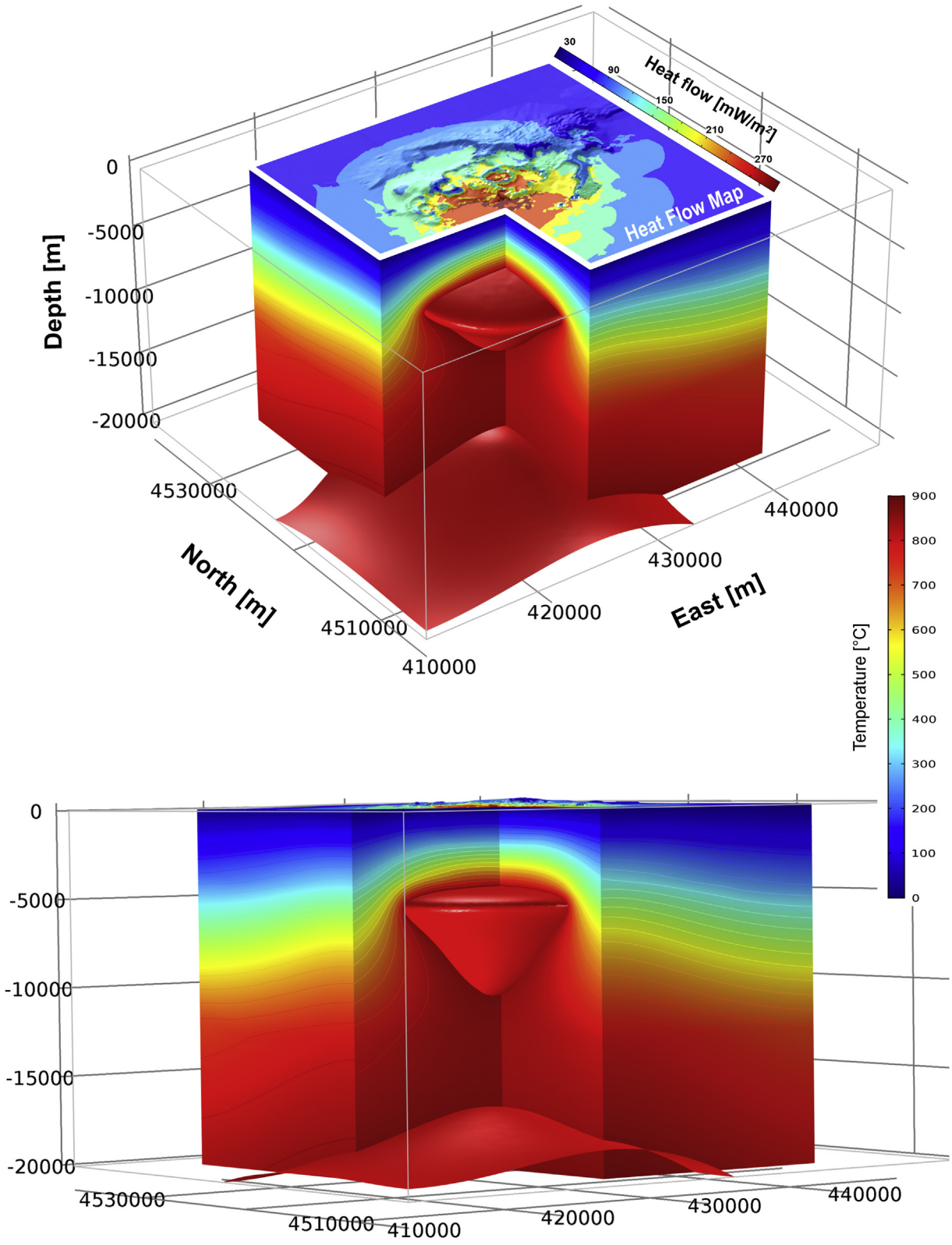

Figure 5. FE model results 2: temperature distribution. Two different 3D views of the modeled temperature. The upper surface of the first panel shows the distribution of the modeled heat flow. The 800 °C isotherm is drawn.

where σ_1 (Pa) and σ_3 (Pa) are maximum and minimum compressive stresses respectively, ρ (kg/m^3) is the density of the material, g (m/s^2) is the acceleration due to gravity, z (m) is the depth, λ (−) is the pore fluid factor, and β (−) is a parameter that depends on the type of faulting (3.0, 1.2 and 0.75 for thrust, strike−slip and normal faulting, respectively).

At sufficiently high temperatures, the creep strength (i.e., the stress difference necessary to achieve a given strain rate) strongly

Please cite this article in press as: Castaldo, R., et al., The impact of crustal rheology on natural seismicity: Campi Flegrei caldera case study, Geoscience Frontiers (2018), https://doi.org/10.1016/j.gsf.2018.02.003

depends on temperature. This regime is empirically described by a power–law creep (Kirby, 1983):

$$(\sigma_1 - \sigma_3)_D = (\dot{\varepsilon}/A)^{1/n} e^{(Q/nRT)} \quad (6)$$

where $\dot{\varepsilon}$ is the strain rate, A ($MPa^{-n}\ s^{-1}$) and n (−) are parameters of the medium, Q (kJ/mol) is the activation energy for creep, R (J/mol K) and T (K) are the gas constant and temperature field distribution, respectively.

By considering the geological and structural information, summarized in section 2, we compute two crustal rheological profiles by using the retrieved thermal field: the first is located in the central part of the CFc, while the second is outside the caldera rim (see Fig. 2 for locations). In Fig. 6 all the solutions for the three β values are shown. However, given that the prevailing faulting regime is extensional, we choose a $\beta = 0.75$ as a representative value of rheological brittle regime at the CFc.

For the sake of completeness, we also present a dataset of 237 focal mechanisms reported in the time interval 1983–2013 (Fig. 6a). They show a scattered distribution with dominance of normal faulting mechanisms, suggesting a predominantly extensional regime, at least at the centre of the caldera which supports the choice of $\beta = 0.75$.

The density distribution $\rho(x,y,z)$ (kg/m^3) varies with depth; the density-depth profile is plotted in Fig. 6b. Ranalli and Murphy (1987) estimated a pore fluid factor (λ) of 0.36. We chose two values of strain rate ε based on the time interval under observation, $10^{-12}\ s^{-1}$, which represents the rate of the phenomenon relative to a time interval of the order of 10^5–10^6 yrs and it is compatible with the starting time of volcanic activity in the Campanian Plain (Brocchini et al., 2001). The second ε value of $10^{-8}\ s^{-1}$ is considered for phenomenon relative to a time interval of 10–100 years, representing a time window of an acquired time-dependent dataset (i.e., deformation, seismicity, temperature). To calculate the B/D transition we used three different values of A, n and Q for the upper crust, lower crust and upper mantle, respectively; these values are listed in Table 3. The rheological profile inside the caldera (Fig. 6b) shows that a shallow B/D transition with ε equal to $10^{-12}\ s^{-1}$ is located at about 4000 m depth. On the contrary, the B/D transition outside the caldera is very deep (15,000–20,000 m), as shown by the rheological profile, and is not influenced heavily by the thermal state and the geological condition of volcanism at the CFc.

Table 3
Physical parameters used to calculate the rheological modeling. A and n are the material creep parameters, and Q is the activation energy for creep behavior (Ranalli, 2001; Solaro et al., 2007).

Layer	A ($MPa^{-n}\cdot s^{-1}$)	n (−)	Q (kJ/mol)
Upper crust (polygenic tufites)	$1.3\cdot10^{-3}$	2.4	220
Lower crust (carbonate badrock and crystalline metamorphic)	$3.2\cdot10^{-3}$	3.2	270
Upper mantle	$1.4\cdot10^{4}$	4.2	450

Recent seismicity at the CFc (1982–2016) is characterized by highly erratic behaviour. The onset of the ground uplift in 1982 was followed, a few months later, by a progressive increase in seismicity in terms of both event occurrence rate and magnitude. Seismicity reached a peak, culminating in the $M = 4.2$ event of October 4th, 1983. Until the end of 1984 its level remained high, with the occurrence of eight events having magnitude range ≥3.8 (D'Auria et al., 2011). At the beginning of 1985, ground uplift reverted to subsidence and seismicity dropped quickly due to the release of stress in the Mofete-Mt. Nuovo area (De Siena et al., 2017). A total of about 16,000 earthquakes were recorded during the interval 1982–1984. In the following decades, ground levels showed almost continuous subsidence until 2005. During this interval three episodes of minor uplift (a few cm) were observed, accompanied by a few small magnitude earthquakes ($M \leq 2.5$). They occurred frequently in 1989, 1994 and 2000, respectively. Since 2005, together with a reversal in the deformation trend, from subsidence to uplift, a moderate increase in the seismicity rate was also observed, consisting of small magnitude earthquakes ($M < 2$), usually clustered within seismic swarms (D'Auria et al., 2011). The last significant swarm occurred on September 7th, 2012; about 200 earthquakes were recorded, the largest with magnitude 1.8.

The spatial distribution of earthquakes during the period under consideration shows two main clusters: one extending from the Solfatara crater to the town of Pozzuoli and the other within the Bay of Pozzuoli (see Fig. 7a and b). According to De Siena et al. (2017), the earthquake cluster beneath Pozzuoli-Solfatara is

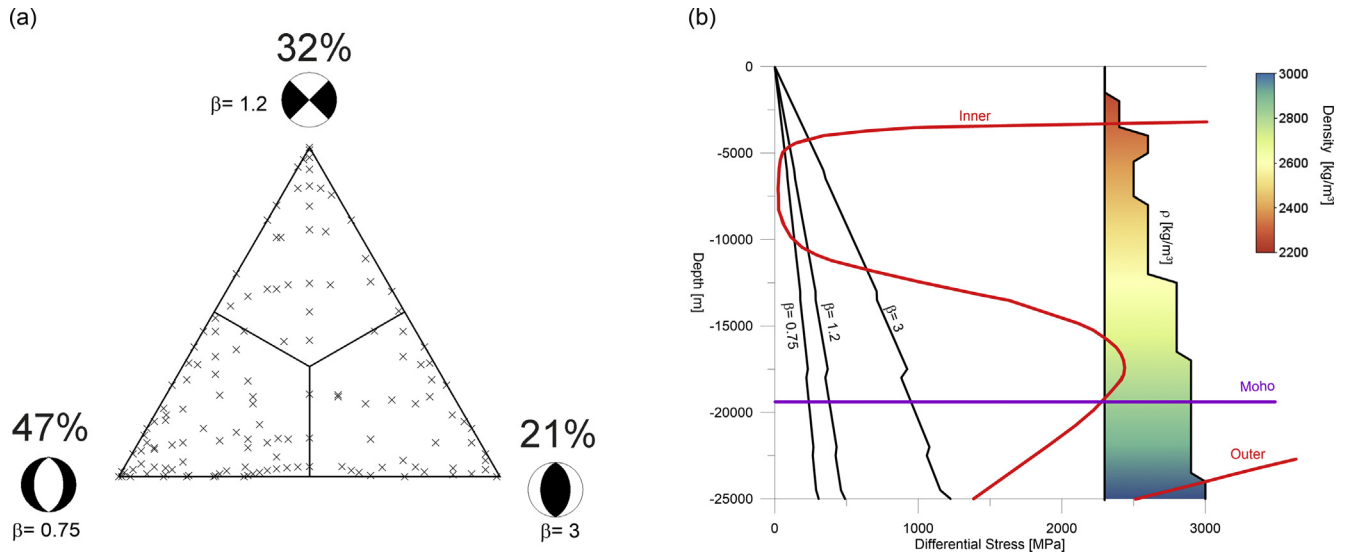

Figure 6. Rheological profile. (a) Triangular diagram built by relating 237 focal mechanisms. (b) Vertical rheological profile where black lines represent three different β values. The image region shows density variation with depth. Red curves show ductile behavior calculated with $\dot{\varepsilon}$ equal to 10^{-12} (s^{-1}) for the inner and outer caldera points (see Fig. 2a for their locations, labeled A and B). Violet line indicates the Mohorovicic discontinuity.

Please cite this article in press as: Castaldo, R., et al., The impact of crustal rheology on natural seismicity: Campi Flegrei caldera case study, Geoscience Frontiers (2018), https://doi.org/10.1016/j.gsf.2018.02.003

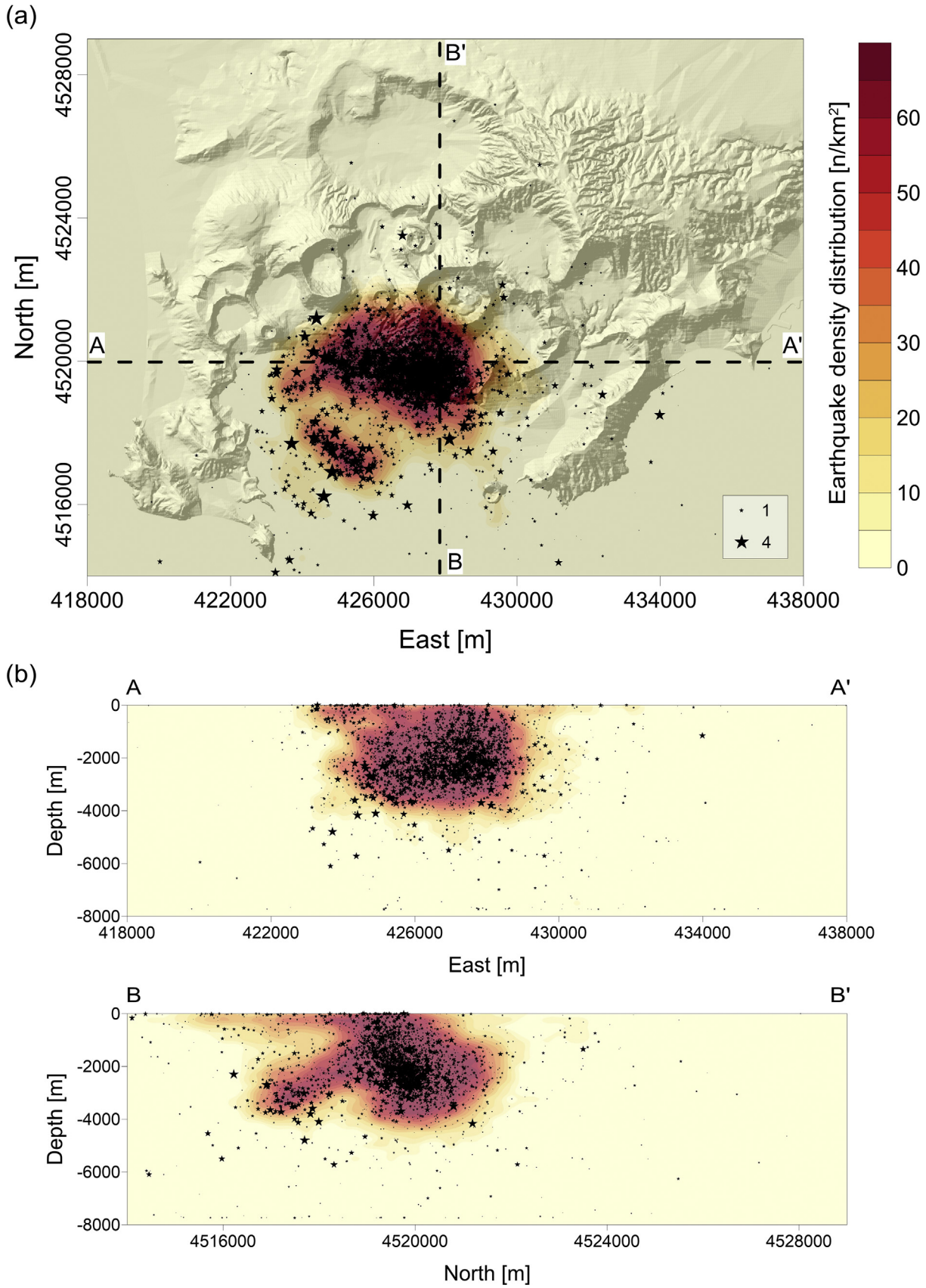

Figure 7. Recent seismicity at the CFc (1982–2016) with $M \geq 1$. (a) Hypocenter density distribution map of natural seismicity (number of events per km^2: n/km^2) superimposed on the CFc SRTM DEM. Black stars represent individual events, with size proportional to event magnitudes. (b) Perpendicular sections, A–A′ and B–B′, highlighting distribution of seismicity with depth.

Please cite this article in press as: Castaldo, R., et al., The impact of crustal rheology on natural seismicity: Campi Flegrei caldera case study, Geoscience Frontiers (2018), https://doi.org/10.1016/j.gsf.2018.02.003

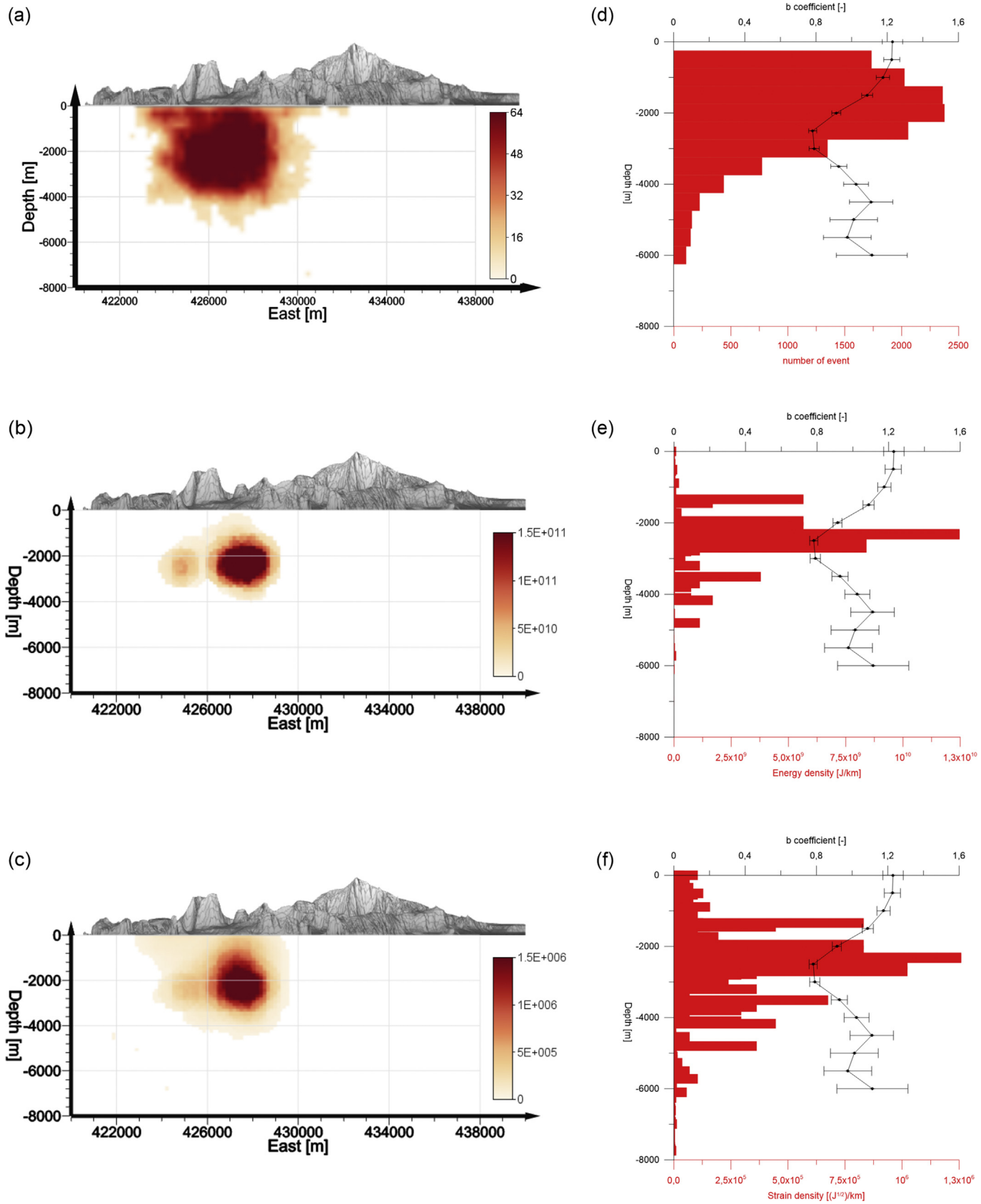

Figure 8. Distribution of event density, strain and energy release. Distribution of the estimated values of (a) number of events per km^2 (n/km^2), (b) energy release (J/km^2) and (c) Benioff strain release (J$^{1/2}$/km^2) reported along the A–A′ cross-section, whose location is shown in Fig. 7a. The shaded surface on the top represents the topography of the DEM SRTM with a vertical exaggeration of 5×. The right panels represent (d) number of events, (e) energy and (f) strain density histograms as functions of depth. The Gutenberg-Richter b-value as a function of depth is represented as a black solid dotted line, with error bars marking its uncertainty.

Please cite this article in press as: Castaldo, R., et al., The impact of crustal rheology on natural seismicity: Campi Flegrei caldera case study, Geoscience Frontiers (2018), https://doi.org/10.1016/j.gsf.2018.02.003

characterized by deeper Pozzuoli earthquakes to shallower Solfatara ones. The depth distributions of the Benioff strain release (Benioff, 1951), of the energy and number of earthquakes (Fig. 8) show clearly that most of the seismicity occurs above 4000 m depth. The b-value curves shown in Fig. 8d–f are computed using earthquakes having magnitudes higher than 1.0. This value is above the magnitude of completeness, which for this catalogue is 0.5 (D'Auria et al., 2011). Uncertainty has been estimated using the formula of Aki (1965). The b-value is 1.2 close to the surface, and decreases reaching a minimum value of 0.8 at a depth of about 2500 m. This minimum occurs at the same depth as the maximum in energy and strain release (Fig. 8b, c, e, f). Lower b-values in volcanic areas have been usually interpreted as consequence of high stress values and/or by highly heterogeneous rocks (Wyss et al., 2001). To better characterize the relationship between seismicity and rheology at the CFc, we show in Fig. 8b and c the distribution of energy and strain, with spatial smoothing using a 1000 m radius filter, along the A–A′ section. The energy and strain distributions clearly show that most of the seismicity occurs beneath the Solfatara crater, with a secondary maximum beneath the town of Pozzuoli. In particular, in the January 1983–December 1984 time interval, microearthquakes nucleated under Pozzuoli and reached vents that were active in the last 5 kyrs, south of Solfatara (De Siena et al., 2017). Accordingly, we argue that from the energy release point of view, the seismicity in the Bay of Pozzuoli is poorly relevant.

The comparison between rheology and seismicity (Fig. 9) shows how earthquake hypocentres are mostly located in the transitional zone of the computed 3D image of B/D for $\varepsilon = 10^{-12}$ s^{-1}. In the case of $\varepsilon = 10^{-8}$ s^{-1} (Fig. 10), the B/D transition is completely below the earthquake hypocentres, i.e., below this zone, the seismicity is very low. This holds true for the CFc, considering both the number of events (Fig. 7a and b) as well as the energy release (Fig. 8b, e). This further suggests that the temperature field, and therefore the rheology, have a strong influence on seismogenetic processes occurring within the CFc.

5. Discussion and conclusions

This work focuses on the development of a 3D FE stationary thermal conductive model in order to investigate the thermo-rheological stratification beneath the CFc by integrating gravity data, seismic reflection profiles and seismic tomography data, and based on an optimization procedure of the geometric heat source parameters.

This approach allowed us to characterize the structural domains of the CFc in terms of thermo-mechanical properties and to define the geometry of the thermal source. We generated several

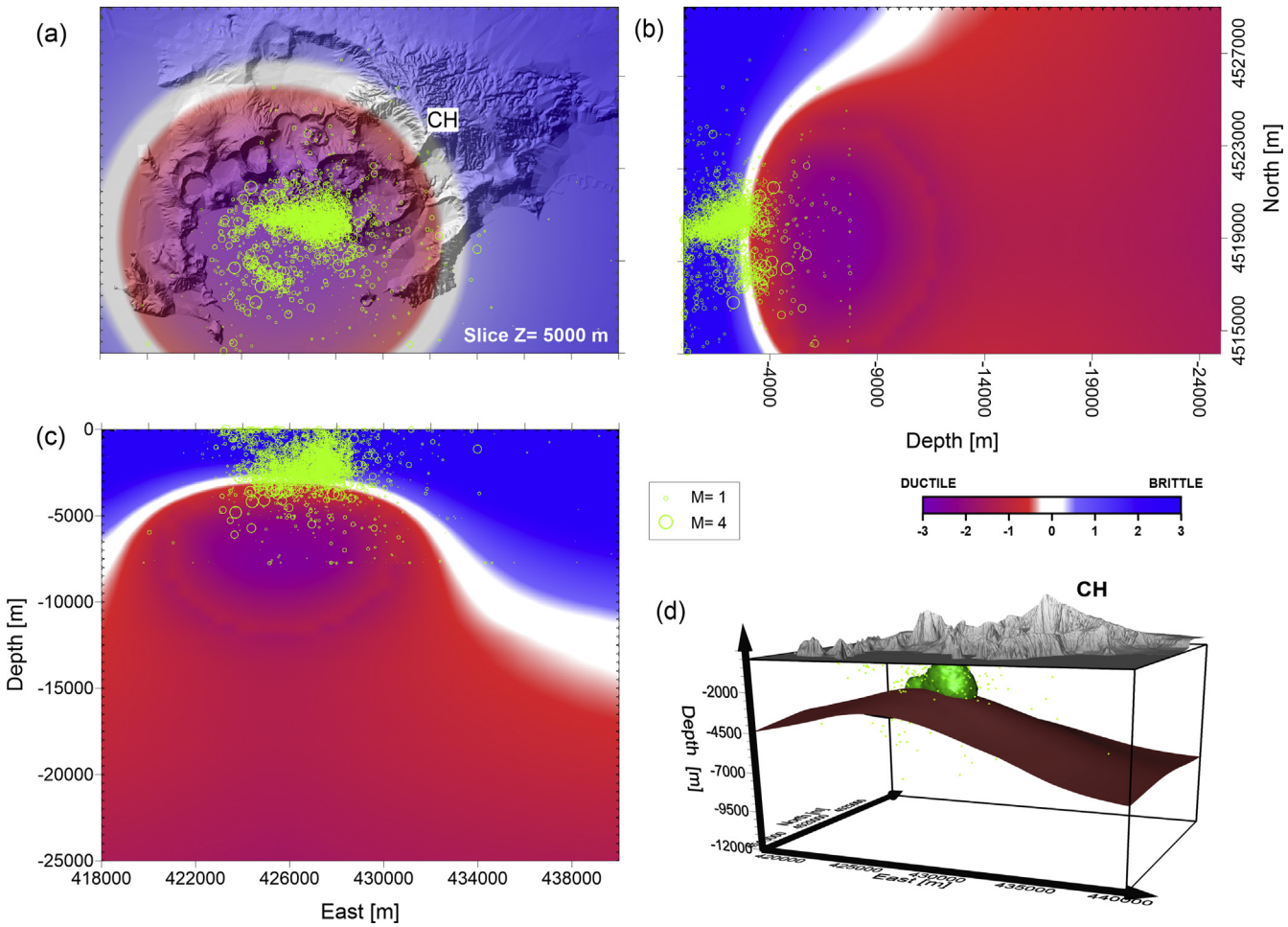

Figure 9. Comparative analysis for $\varepsilon = 10^{-12}$ (s^{-1}). Comparison between the rheological stratification of the crust and seismicity distribution. Ductile and brittle crustal behavior are shown along (a) a horizontal slice at 5000 m depth, (b) A–A′ and (c) B–B′ vertical sections (see Fig. 7a for their locations). Green circles mark hypocenters of earthquakes with $M \geq 1$. (d) The red isovolume of the B/D transition is calculated by considering $\varepsilon = 10^{-12}$ (s^{-1}); the green region represents the energy release density isovolume of 5×10^9 (J/km).

Please cite this article in press as: Castaldo, R., et al., The impact of crustal rheology on natural seismicity: Campi Flegrei caldera case study, Geoscience Frontiers (2018), https://doi.org/10.1016/j.gsf.2018.02.003

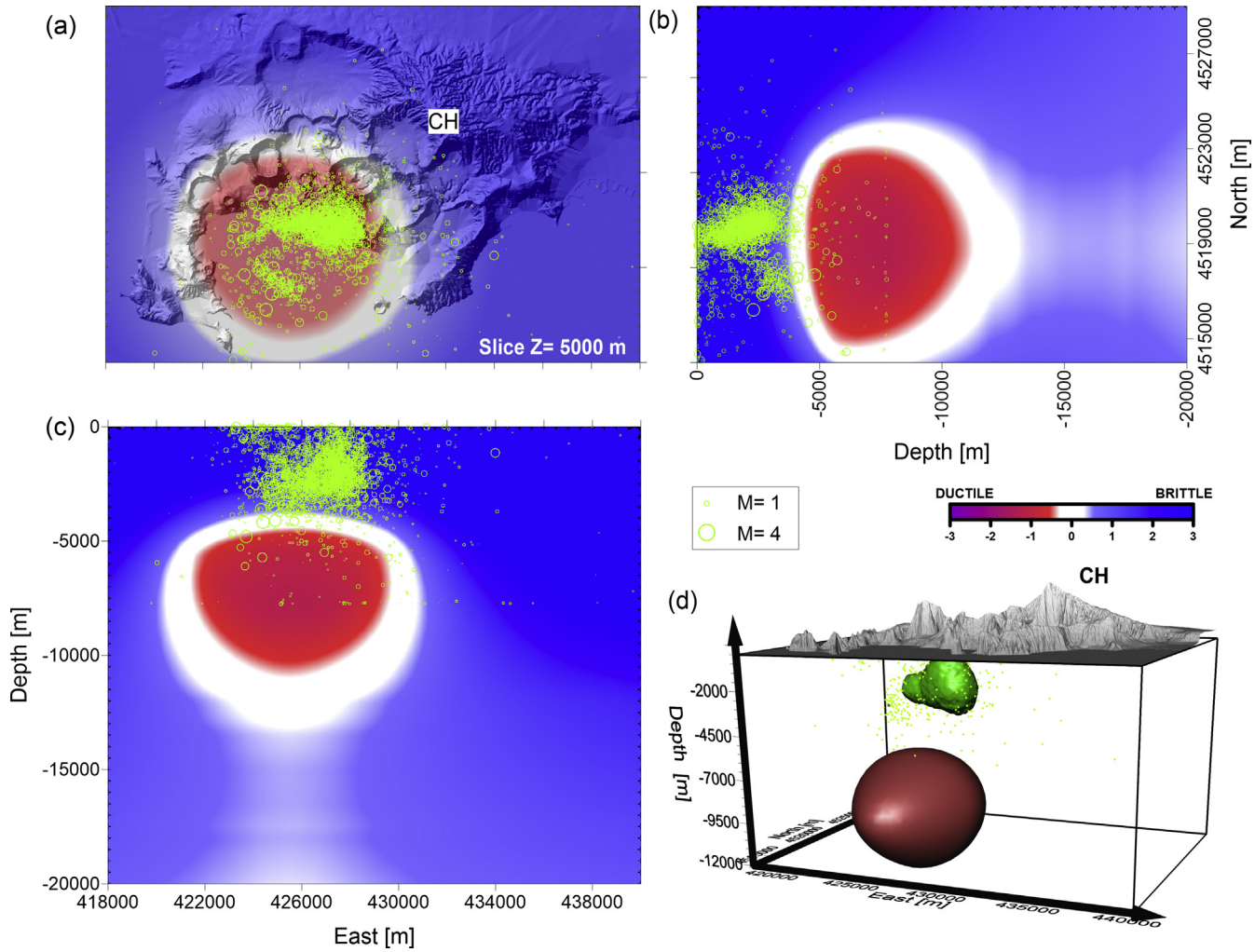

Figure 10. Comparative analysis for $\varepsilon = 10^{-8}$ (s^{-1}). Comparison between the rheological stratification of the crust and natural seismicity. Ductile and brittle crustal behavior are shown along (a) a horizontal slice at 5000 m depth, (b) A–A′ and (c) B–B′ vertical sections (see Fig. 7a for their locations). Green circles mark hypocenters of earthquakes with $M \geq 1$. (d) The red isovolume of the B/D transition is calculated by considering $\varepsilon = 10^{-8}$ (s^{-1}); the green region represents the energy release density isovolume of 5×10^9 (J/km).

forward models consisting of a 3D stationary conductive solution of the CFc thermal field. The use of the optimization procedure, based on a Monte Carlo method, allowed us to find a good fit among the available borehole temperatures, heat flow measurements and FE model results. In particular, we calibrated the model by exploiting nine deep geothermal wells and ten heat flow measurements. We found major discrepancies between the retrieved thermal model and measured data in the Mofete area, about 6000 m west of the caldera center. Several hypothesis could be offered to interpret these discrepancies: (1) the effect of shallow hydrothermal activity as suggested by mineralogical studies (De Vivo et al., 1989; Chiodini et al., 2010; Mormone et al., 2015), (2) the lateral variations in thermal conductivity distribution used in our model (Wohletz et al., 1999; Carlino et al., 2013) and (3) the impact of advective components on the thermal state, likely due to the existence of structures related to the boundary of the NYT caldera; the last aspect could explain the anomalous behavior with respect to our conductive model results. According to De Siena et al. (2017), the fumarole at Mofete could be evidence of advective heat transport through the fractured zone (where micro-earthquakes occurred) that connects the 3–4 km deep reservoir to the surface.

The estimated best source geometric parameters indicate the presence of a heat source, extending horizontally for about 7 km, with a flat top and located at about 5 km depth. Thermal modelling led to the definition of a 3D B/D transition zone for different time scales: 10^5–10^6 years ($\varepsilon = 10^{-12}$ s^{-1}) corresponding to the time evolution of the caldera, and 10–100 years ($\varepsilon = 10^{-8}$ s^{-1}), corresponding to recent phenomena observed at the CFc. We found that the B/D transition associated with the shorter scale agrees well with the present distribution of hypocenters, which are mostly clustered above 4000 m (more than 90%); this is also clearly evidenced by the spatial distribution of the strain and energy release, which reaches a maximum at about 2000 m depth and becomes negligible below 3000 m, making the estimated volume of the ductile region about 180×10^9 m^3. Similar shallow cut-offs of natural seismicity have also been noted at other volcanoes (Ito, 1993). For instance, in large silicic calderas, the seismicity is usually confined to relatively shallow depths, e.g. Long Valley (Prejean et al., 2002), Rabaul (Mori and McKee, 1987) and Taupo (Bryan et al., 1999). This feature is taken to an extreme at the Yellowstone caldera, where seismicity is nearly absent within the caldera (DeNosaquo et al., 2009). This feature is commonly interpreted as a thermal "*signature*" of large magmatic

Please cite this article in press as: Castaldo, R., et al., The impact of crustal rheology on natural seismicity: Campi Flegrei caldera case study, Geoscience Frontiers (2018), https://doi.org/10.1016/j.gsf.2018.02.003

bodies, whose heat flow heavily distorts the shape of the B/D transition in the surrounding crust. However, this behaviour deviates from the seismicity pattern observed at many stratovolcanoes. The seismicity at these volcanoes is typically confined to a highly elongated volume extending up to depths of more than 10,000 m, e.g., at Mt. Spurr (up to 13 km), Mt. Vesuvius (up to 7 km) (D'Auria et al., 2012) and at the Merapi volcano (Ratdomopurbo and Poupinet, 2000). This probably reflects the ephemeral nature of the magma chambers associated with these volcanoes, since they are unable to significantly perturb the rheology of the surrounding crust.

The results from our study, relevant to the rheology stratification and the crustal seismogenic volume, are in good agreement with a recent study by Di Vito et al. (2016), which highlighted the presence of an oblate magma reservoir at an analogous depth below the CFc. Another study by De Siena et al. (2017) showed that a zone of high seismic attenuation between 4 and 4.5 km depth can exist in rocks overlying a magmatic anomaly with high heating potential. Doglioni et al. (2014) proposed that natural seismicity can occur within the brittle region, which we identify in our modelling results.

The retrieved picture of the B/D transition evaluated by considering the shortest time scale (Fig. 10) has important implications in constraining potential seismogenic volumes. Indeed, the inferred depth of 4000 m (for $\varepsilon = 10^{-8}$ s^{-1}) implies that a fault spanning the whole caldera (maximum breadth of about 11,000 m, along the E–W direction) with a stress drop of 4 bar (De Natale et al., 1987) would result in an event with magnitude of about M_w 5.1. However, because of its highly fractured structure, such a long seismic rupture (fault area) is unrealistic for the CFc, at least in pre-eruptive conditions (Festa et al., 2004). A more conservative fault area (i.e. 4000 m × 3000 m) suggests that a magnitude M_w 4.7 event is a realistic estimate for the upper limit of pre-eruptive earthquakes at the CFc (Convertito and Zollo, 2011).

Acknowledgement

This work was carried out within the framework of the GEOTHERMAL ATLAS OF SOUTHERN ITALY project, one of six constituting the program CNR per il Mezzogiorno of the Italian National Research Council, aimed at improving know-how in the fields of advanced technology for energy efficiency, environmental protection, agro-food innovative methodologies for the Made in Italy and biotech medicine production, and was partially funded by 368 DTA. AD004.065.001 Geophysics – Project CNR _PDGP 2016-2018.

Appendix A. Supplementary data

Supplementary data related to this article can be found at https://doi.org/10.1016/j.gsf.2018.02.003.

References

Agip, 1987. Geotermia Produzione e Utilizzazioni. AGIP Editor. San Donato, 23 pp.
Aki, K., 1965. Maximum likelihood estimate of b in the formula log N=a-bM and its confidence limits. Bulletin of the Earthquake Research Institute Tokyo University 43, 237–239.
Avallone, A., Zollo, A., Briole, P., Delacourt, C., Beauducel, F., 1999. Subsidence of Campi Flegrei (Italy) detected by SAR interferometry. Geophysical Research Letters 26 (15), 2303–2306.
Benioff, H., 1951. Earthquakes and rock creep, part I: creep characteristics of rocks and the origin of aftershocks. Bulletin of the Seismological Society of America 41, 31–62.
Berrino, G., Corrado, G., Riccardi, U., 2008. Sea gravity data in the Gulf of Naples. A contribution to delineating the structural pattern of the Phlegraean Volcanic District. Journal of Volcanology and Geothermal Research 175, 241–252.
Bianchi, R., Coradini, C., Federico, C., Giberti, G., Lanciano, P., Pozzi, J.P., Sartoris, G., Scandone, R., 1987. Modeling of surface deformations in volcanic areas. The 1970–72 and 1982–84 crises of Campi Flegrei, Italy. Journal of Geophysical Research 92, 14139–14150.
Brocchini, D., Principe, C., Castratori, D., Laurenzi, M.A., Gorla, L., 2001. Quaternary evolution of the sector of the Campanian Plain and Somma-Vesuvius early activity: trecase 1 well insight. Mineralogy and Petrology 73, 67–91.
Bryan, C.J., Sherburn, S., Bibby, H.M., Bannister, S.C., Hurst, A.W., 1999. Shallow seismicity of the central Taupo Volcanic Zone, New Zealand: its distribution and nature. New Zealand Journal of Geology and Geophysics 42, 533–542.
Carlino, S., Somma, R., Troise, C., De Natale, G., 2013. The geothermal exploration of Campanian volcanoes: historical review and future development. Renewable and Sustainable Energy Reviews 16, 1004–1030. https://doi.org/10.1016/j.rser.2011.09.023.
Castaldo, R., Gola, G., Santilano, A., De Novellis, V., Pepe, S., Manzo, M., Manzella, A., Tizzani, P., 2017. The role of thermo-rheological properties of the crust beneath Ischia Island (Southern Italy) in the modulation of the ground deformation pattern. Journal of Volcanology and Geothermal Research 344, 154–173, 15 September 2017.
Chapman, D.S., Furlong, K.P., 1992. In: Fountain, D.M., Arculus, R.J., Kay, R.M. (Eds.), Continental Lower Crust. Elsevier Science, Amsterdam, pp. 179–199.
Chelini, W., Sbrana, A., 1987. Subsurface geology. In: Rosi, M., Sbrana, A. (Eds.), Phlegrean Fields. CNR Quaderni de "La Ricerca Scientifica", vol. 114, pp. 94–103.
Chiarabba, C., Moretti, M., 2006. An insight into the unrest phenomena at the Campi Flegrei caldera from Vp and Vp/Vs tomography. Terra Nova 18 (6), 373–379. https://doi.org/10.1111/j.1365-3121.2006.00701.x.
Chiodini, G., Caliro, S., Cardellini, C., Granieri, D., Avino, R., Baldini, A., Donnini, M., Minopoli, C., 2010. Long term variations of the Campi Flegrei (Italy) volcanic system as revealed by the monitoring of hydrothermal activity. Journal of Geophysical Research 115, B03205. https://doi.org/10.1029/2008JB006258.
Chiodini, G., Paonita, A., Aiuppa, A., Costa, A., Caliro, S., De Martino, P., Acocella, V., Vandemeulebrouck, J., 2016. Magmas near the critical degassing pressure drive volcanic unrest towards a critical state. Nature Communications 7, 13712. https://doi.org/10.1038/ncomms13712.
Civetta, L., Carluccio, E., Innocenti, F., Sbrana, A., Taddeucci, G., 1991. Magma chamber evolution at Phlegrean Fields during the last 10 ka, in the light of trace elements and isotope composition. European Journal of Mineralogy 3, 415–428.
Convertito, V., Zollo, A., 2011. Assessment of pre-crisis and syn-crisis seismic hazard at Campi Flegrei and Mt. Vesuvius volcanoes, Campania, southern Italy. Bulletin of Volcanology 73, 767–783. https://doi.org/10.1007/s00445-011-0455-2.
Corrado, G., De Lorenzo, S., Mongelli, F., Tramacere, A., Zito, G., 1998. Surface heat flow density at the Phlegrean Fields Caldera Southern Italy. Geothermics 27 (4), 469–484.
De Lorenzo, S., Zollo, A., Mongelli, F., 2001. Source parameters and three-dimensional attenuation structure from the inversion of microearthquake pulse width data: Qp imaging and inference on the thermal state of the Campi Flegrei caldera (southern Italy). Journal of Geophysical Research 106 (B8), 16265–16286.
De Natale, G., Iannaccone, G., Martini, M., Zollo, A., 1987. Seismic sources and attenuation properties at the Campi Flegrei volcanic area. Pure and Applied Geophysics 125 (6), 883–917.
De Natale, G., Zollo, A., Ferraro, A., Virieux, J., 1995. Accurate fault mechanism determinations for a 1984 earthquake swarm at Campi Flegrei caldera (Italy) during an unrest episode: implications for volcanological research. Journal of Geophysical Research 100, 24167–24185.
De Siena, L., Chiodini, G., Vilardo, G., Del Pezzo, E., Castellano, M., Colombelli, S., Tisato, N., Ventura, G., 2017. Source and dynamics of a volcanic caldera unrest: Campi Flegrei, 1983–84. Scientific Reports 7. https://doi.org/10.1038/s41598-017-08192-7. Article number: 8099(2017).
De Vivo, B., Belkin, H.E., Barbieri, M., Chelini, W., Lattanzi, P., Lima, A., Tolomeo, L., 1989. The Campi Flegrei (Italy) geothermal system: a fluid inclusion study of the Mofete and San Vito fields. Journal of Volcanology and Geothermal Research 36, 303–326.
Del Gaudio, C., Aquino, I., Ricciardi, G.P., Ricco, C., Scandone, R., 2010. Unrest episodes at Campi Flegrei: a reconstruction of vertical ground movements during 1905–2009. Journal of Volcanology and Geothermal Research 195 (1), 48–56. https://doi.org/10.1016/j.jvolgeores.2010.05.014.
DeNosaquo, K., Smith, R.B., Lowry, A.R., 2009. Density and lithospheric strength models of the Yellowstone-Snake River Plain volcanic system from gravity and heat flow data. Journal of Volcanology and Geothermal Research 188, 108–127. https://doi.org/10.1016/j.jvolgeores.2009.08.006.
Di Vito, M.A., Isaia, R., Orsi, G., Southon, J., De Vita, S., D'Antonio, M., Pappalardo, L., Piochi, M., 1999. Volcanic and deformational history of the Campi Flegrei caldera in the past 12 ka. Journal of Volcanology and Geothermal Research 91, 221–246.
Di Vito, M.A., Acocella, V., Aiello, G., Barra, D., Battaglia, M., Carandente, A., Del Gaudio, C., de Vita, S., Ricciardi, G.P., Ricco, C., Scandone, R., Terrasi, F., 2016. Magma transfer at Campi Flegrei caldera (Italy) before the 1538 AD eruption. Scientific Reports 6, 32245. https://doi.org/10.1038/srep32245.
Doglioni, C., Barba, S., Carminati, E., Riguzzi, F., 2014. Role of the brittle–ductile transition on fault activation. Physics of the Earth and Planetary Interiors 184, 160–171.

D'Antonio, M., Civetta, L., Orsi, G., Pappalardo, L., Piochi, M., Carandente, A., De Vita, S., Di Vito, M.A., Isaia, R., Southon, J., 1999. The present state of the magmatic system of the Campi Flegrei caldera based on the reconstruction of its behaviour in the past 12 ka. Journal of Volcanology and Geothermal Research 91, 247–268.

D'Auria, L., Giudicepietro, F., Aquino, I., Borriello, G., Del Gaudio, C., Lo Bascio, D., Martini, M., Ricciardi, G., Ricciolino, P., Ricco, C., 2011. Repeated fluid-transfer episodes as a mechanism for the recent dynamics of Campi Flegrei caldera (1989–2010). Journal of Geophysical Research 116, B04313. https://doi.org/10.1029/2010JB007837.

D'Auria, L., Giudicepietro, F., Martini, M., Lanari, R., 2012. The 4D imaging of the source of ground deformation at Campi Flegrei caldera (southern Italy). Journal of Geophysical Research 117, B08209. https://doi.org/10.1029/2012JB009181.

Fedi, M., Nunziata, C., Rapolla, A., 1991. The Campania-Campi Flegrei area: a contribution to discern the best structural model from gravity interpretation. Journal of Volcanology and Geothermal Research 48, 51–59.

Ferrucci, F., Gaudiosi, G., Pino, N.A., Luongo, G., Hirn, A., Mirabile, L., 1986. Seismic detection of a major moho upheaval beneath the Campanian volcanic area. Geophysical Research Letters 16 (11), 1317–1320.

Ferrucci, F., Hirn, A., De Natale, G., Virieux, J., Mirabile, L., 1992. P-SV conversions at a shallow boundary beneath Campi Flegrei Caldera (Italy): evidence for the magma chamber. Journal of Geophysical Research 97, 15351–15359.

Festa, G., Zollo, A., Manfredi, G., Polese, M., Cosenza, E., 2004. Simulation of earthquake ground motion and effects on engineering structures during the preeruptive phase of an active volcano. Bulletin of the Seismological Society of America 94 (6), 2213–2221.

Goetze, C., Evans, B., 1979. Stress and temperature in the bending lithosphere as constrained by experimental rock mechanics. Geophysical J. R. Astronomical Society 59, 463–478.

Goovaerts, P., 1997. Geostatistics for Natural Resources Evaluation. Oxford University Press.

Ito, K., 1993. Cutoff depth of seismicity and large earthquakes near active volcanoes in Japan. Tectonophysics 217, 11–21.

Kirby, S.H., 1983. Rheology of the lithosphere. Reviews of Geophysics 21 (6), 1458–1487.

Lundgren, P., Usai, S., Sansosti, E., Lanari, R., Tesauro, M., Fornaro, G., Berardino, P., 2001. Modeling surface deformation observed with synthetic aperture radar interferometry at Campi Flegrei caldera. Journal of Geophysical Research 106, 19355–19366.

Luongo, G., Cubellis, E., Obrizzo, F., Petrazzuoli, S.M., 1991. The mechanics of the Campi Flegrei resurgent caldera – a model. Journal of Volcanology and Geothermal Research 45, 161–172.

Meissner, R., Strehlau, J., 1982. Limits of stresses in continental crusts and their relation to the depth-frequency distribution of shallow earthquakes. Tectonics 1 (1), 73–89. https://doi.org/10.1029/TC001i001p00073.

Mori, J., McKee, C., 1987. Outward-dipping ring-fault structure at Rabaul caldera as shown by earthquake locations. Science 235, 193–195.

Mormone, A., Troise, C., Piochi, M., Balassone, G., Joachimski, M., De Natale, G., 2015. Mineralogical, geochemical and isotopic features of tuff from the CFDDP 506 m hole: hydrothermal activity in the eastern side of the Campi Flegrei volcano (southern Italy). Journal of Volcanology and Geothermal Research 290, 39–52. https://doi.org/10.1016/j.jvolgeores.2014.12.003.

Ord, A., Hobbs, B.E., 1989. The strength of the continental crust, detachment zones and the development of plastic instabilities. Tectonophysics 158, 269–289.

Orsi, G., Civetta, L., Del Gaudio, C., de Vita, S., Di Vito, M.A., Isaia, R., Petrazzuoli, S.M., Ricciardi, G.P., Ricco, C., 1999. Short-term ground deformations and seismicity in the resurgent Campi Flegrei caldera (Italy): an example of active block-resurgence in a densely populated area. Journal of Volcanology and Geothermal Research 91, 415–451.

Ortiz, R., Arana, V., Astiz, M., Valentin, A., 1984. Magnetotelluric survey in the brady seismic area of Campi Flegrei. Bulletin of Volcanology 47, 239–246.

Pappalardo, L., Civetta, L., D'Antonio, M., Deino, A., Di Vito, M.A., Orsi, G., Carandente, A., de Vita, S., Isaia, R., Piochi, M., 1999. Chemical and isotopical evolution of the Phlegraean magmatic system before the Campanian Ignimbrite (37 ka) and the Neapolitan Yellow Tuff (12 ka) eruptions. Journal of Volcanology and Geothermal Research 91, 141–166.

Prejean, S., Ellsworth, W., Zoback, M., Waldhauser, F., 2002. Journal of Geophysical Research 107 (B12), 2355. https://doi.org/10.1029/2001JB001168.

Ranalli, G., 2001. Rheology of the Earth, second ed. Chapman & Hall, London.

Ranalli, G., Murphy, D., 1987. Rheological stratification of the lithosphere. Tectonophysics 132, 281–295.

Ratdomopurbo, A., Poupinet, G., 2000. An overview of the seismicity of Merapi volcano (Java, Indonesia), 1983–1994. Journal of Volcanology and Geothermal Research 100, 193–214.

Rosi, M., Sbrana, A., 1987. Phlegrean fields, introduction, geological setting of the area, stratigraphy, description of mapped products, petrography, tectonics. Quaderni de "La Ricerca Scientifica" Consiglio Nazionale delle Ricerche 114, 9–93.

Scarpati, C., Perrotta, A., Lepore, S., Calvert, A., 2013. Eruptive history of Neapolitan volcanoes: constraints from 40Ar–39Ar dating. Geological Magazine 150 (3), 412–425. https://doi.org/10.1017/S0016756812000854.

Sen, M.K., Stoffa, P.L., 2013. Global Optimization Methods in Geophysical Inversion, second ed. Cambridge University Press.

Sibson, R.H., 1974. Frictional constraints on thrust, wrench and normal faults. Nature 249, 542–544.

Smith, V.C., Isaia, R., Pearce, N.J.G., 2011. Tephrostratigraphy and glass compositions of post-15 kyr Campi Flegrei eruptions: implications for eruption history and chronostratigraphic markers. Quaternary Science Reviews 30, 3638–3660.

Solaro, G., Tizzani, P., Milano, G., Pauselli, C., 2007. Rheological behaviour of the crust in Southern Apennine (Italy): results from a thermal and seismological study. Terra Nova 19, 353–359.

Trasatti, E., Casu, F., Giunchi, C., Pepe, S., Solaro, G., Tagliaventi, S., Berardino, P., Manzo, M., Pepe, A., Ricciardi, G.P., Sansosti, E., Tizzani, P., Zeni, G., Lanari, R., 2008. The 2004–2006 uplift episode at Campi Flegrei Caldera (Italy): constraints from SBAS-DInSAR ENVISAT data and Bayesian source inference. Geophysical Research Letters 35 (L07308). https://doi.org/10.1029/2007GL033091.

Turcotte, D.L., Schubert, G., 2002. Geodynamics, second ed. Cambridge University Press.

Villemant, B., 1988. Trace element evolution in the Phlegrean Fields (Central Italy): fractional crystallization and selective enrichment. Contributions to Mineralogy and Petrology 98, 169–183.

Wohletz, K., Civetta, L., Orsi, G., 1999. Thermal evolution of the Phlegraean magmatic system. Journal of Volcanology and Geothermal Research 91 (381), 414.

Wyss, M., Klein, F., Nagamine, K., Wiemer, S., 2001. Anomalously high B-values in the South Flank of Kilauea volcano, Hawaii- evidence for the distribution of magma below Kilauea's east rift zone. Journal of Volcanology and Geothermal Research 106, 23–37.

Zhang, Z., Zhu, J.Z., 1998. Analysis of the super convergent patch recovery technique and a posteriori error estimator in the finite element method (II). Computer Methods in Applied Mechanics and Engineering 163 (1–4), 159–170. https://doi.org/10.1016/S0045-7825(98)00010-3.

Please cite this article in press as: Castaldo, R., et al., The impact of crustal rheology on natural seismicity: Campi Flegrei caldera case study, Geoscience Frontiers (2018), https://doi.org/10.1016/j.gsf.2018.02.003